Deletion of the *H19* differentially methylated domain results in loss of imprinted expression of *H19* and *Igf2*

Joanne L. Thorvaldsen, Kristen L. Duran, and Marisa S. Bartolomei[1]

Howard Hughes Medical Institute and Department of Cell and Developmental Biology, University of Pennsylvania School of Medicine, Philadelphia, Pennsylvania 19104 USA

Differentially methylated sequences associated with imprinted genes are proposed to control genomic imprinting. A 2-kb region located 5′ to the imprinted mouse *H19* gene is hypermethylated on the inactive paternal allele throughout development. To determine whether this differentially methylated domain (DMD) is required for imprinted expression at the endogenous locus, we have generated mice harboring a 1.6-kb targeted deletion of the DMD and assayed for allelic expression of *H19* and the linked, oppositely imprinted *Igf2* gene. *H19* is activated and *Igf2* expression is reduced when the DMD deletion is paternally inherited; conversely, upon maternal transmission of the mutation, *H19* expression is reduced and *Igf2* is activated. Consistent with the DMD's hypothesized role of setting up the methylation imprint, the mutation also perturbs allele-specific methylation of the remaining *H19* sequences. In conclusion, these experiments show that the *H19* hypermethylated 5′ flanking sequences are required to silence paternally derived *H19*. Additionally, these experiments demonstrate a novel role for the DMD on the maternal chromosome where it is required for the maximal expression of *H19* and the silencing of *Igf2*. Thus, the *H19* differentially methylated sequences are required for both *H19* and *Igf2* imprinting.

[*Key Words*: Differentially methylated domain; DNA methylation; *H19*; *Igf2*; genomic imprinting]

Received September 3, 1998; revised version accepted October 8, 1998.

The imprinted, maternally expressed mouse *H19* gene is located in proximity to a number of imprinted genes on the distal portion of mouse chromosome 7 (Bartolomei et al. 1991; Caspary et al. 1998). Other genes in the region include the paternally expressed *insulin-like growth factor 2* (*Igf2*) and *insulin 2* (*Ins2*) genes and the maternally expressed $p57^{KIP2}$, *Kvlqt1*, and *Mash2* genes (DeChiara et al. 1991; Giddings et al. 1994; Guillemot et al. 1995; Hatada and Mukai 1995; Gould and Pfeifer 1998). A conserved cluster of imprinted genes is found on human chromosome 11p15.5 in the Beckwith–Wiedemann syndrome critical region (Reid et al. 1997). A second cluster of imprinted genes resides in the Prader-Willi and Angelman syndrome critical regions on human chromosome 15, with the syntenic region located centrally on mouse chromosome 7 (Nicholls et al. 1998). Given the intriguing clustering of imprinted genes, it has been proposed that the imprinting of individual genes is dependent upon their linkage to other imprinted genes (Barlow 1997; Bartolomei and Tilghman 1992, 1997).

The interdependence of imprinted genes has been demonstrated clearly for the mouse *H19* and *Igf2* genes. The mouse *H19* gene is highly expressed, does not encode a protein product, and is located 75 kb from the gene encoding the fetal mitogenic protein IGFII (Zemel et al. 1992). It has been shown that the expression of these two genes is, in part, dependent upon competition for two endodermal-specific enhancers that are located +9 and +11 kb relative to the start of *H19* transcription (Yoo-Warren et al. 1988). Deletion of these enhancers on the maternal chromosome results in a loss of *H19* expression in endodermal tissues, whereas deletion of the enhancers on the paternal chromosome results in the corresponding loss of *Igf2* expression (Leighton et al. 1995b). Additionally, deletion of the *H19* structural gene and 10 kb of upstream flanking sequence from the maternal allele leads to expression of the normally repressed *Igf2* gene, indicating that the enhancers which initially supported maternally derived *H19* expression were free to enhance the expression of *Igf2* (Leighton et al. 1995a).

Whereas the imprinted expression of *Igf2* is dependent upon linkage to the *H19* locus, the imprinting of *H19* appears to be autonomous. This idea is supported by *H19* transgenic experiments in which constructs harboring 4 kb of upstream flanking sequence, an internally deleted *H19* structural gene and the 3′ endodermal enhancers are imprinted similarly to the endogenous gene (Bartolomei et al. 1993; Pfeifer et al. 1996; Elson and Bartolomei

[1]**Corresponding author.**
E-MAIL bartolom@mail.med.upenn.edu; FAX (215) 573-6434.

1997). We have proposed that this autonomous regulation is governed by paternal-specific DNA methylation present at the endogenous and transgenic loci (Bartolomei et al. 1993). The 7 kb of paternal-specific methylation observed in somatic tissues and sperm includes 4 kb of upstream flanking sequence and the *H19* structural gene (Bartolomei et al. 1993; Brandeis et al. 1993; Ferguson-Smith et al. 1993). The importance of methylation for the repression of the paternal allele of *H19* is underscored by experiments in which imprinted gene expression was characterized in mice that were deficient for the DNA methyltransferase gene *Dnmt1* (Li et al. 1993). When analyzed prior to their death, *Dnmt1* null mice expressed both alleles of *H19*, suggesting that DNA methylation is at least required to maintain *H19* imprinting. To demonstrate that DNA methylation could also serve a causative role in the marking of the parental alleles and the setting of the parental imprint, we assayed DNA methylation of *H19* during embryogenesis, with an emphasis on preimplantation development as this is the time when the embryo undergoes a period of generalized demethylation (Monk et al. 1987; Sanford et al. 1987). A 2-kb region located from −2 to −4 kb relative to the start of transcription is methylated exclusively on the paternal allele throughout development, suggesting that this region is crucial to determining the imprinted expression of *H19* (Tremblay et al. 1995, 1997). When this region was deleted from the original imprinted *H19* transgene, the new transgenes were expressed and hypomethylated regardless of parental origin (Elson and Bartolomei 1997).

To determine the role of the 2-kb differentially methylated domain (DMD) at the endogenous *H19* locus, we have generated mice lacking the DMD. When the DMD deletion allele is transmitted to the progeny from the father, the normally repressed paternal *H19* allele is activated and the expression of the linked paternal *Igf2* gene is reduced coordinately. In contrast, transmission of the mutant *H19* allele by the mother results in reduced expression of the *H19* gene with a concomitant activation of the maternal *Igf2* allele, revealing a novel regulatory role for this region. Whereas these experiments prove that the DMD is necessary for silencing the paternal *H19* allele, they also show that the DMD is essential on the maternal chromosome for the exclusive expression of *H19* and the silencing of *Igf2*. We conclude that the DMD is required on both parental alleles for the reciprocal imprinting of *H19* and *Igf2*.

Results

Targeted disruption of the H19 *upstream differentially methylated domain*

The region from approximately −2 to −4 kb relative to the start of *H19* transcription is methylated in sperm, unmethylated in oocytes, and preferentially methylated on the paternal allele throughout development (Tremblay et al. 1995, 1997; Olek and Walter 1997). To test the role of this DMD at the endogenous locus, we deleted most of the DMD by gene targeting in embryonic stem (ES) cells and generated mice with the deletion. As shown in Figure 1b, a targeting vector was constructed in which 1.6 kb of the DMD was replaced by the neomycin resistance (*neo*^{r}) gene flanked by loxP sites. The deletion removes 48 of the CpG dinucleotides that we have proposed to be essential for conferring imprinted expression (Tremblay et al. 1995, 1997). The remaining DMD sequence includes five differentially methylated CpG dinucleotides located 5′ to the targeted deletion.

Because the function of a putative imprinting regulatory element was being tested, it was important to eliminate any new regulatory elements introduced by the *neo*^{r} gene cassette. Therefore, following the identification of correctly targeted cells lines, two independent clones were chosen for a second electroporation with a vector encoding Cre recombinase to derive clones that deleted the *neo*^{r} gene (Fig. 1c,d). Cells (with and without the *neo*^{r} gene) were injected into C57BL/6J host blastocysts and mice inheriting the targeted allele were selected for subsequent breeding. The mutant mice were maintained by breeding to C57BL/6J mice. For analysis of allelic imprinting patterns, the heterozygous DMD mutant mice were mated with a strain of mice [B6(CAST–*H19*), (Tremblay et al. 1995)] in which the portion of distal chromosome 7 harboring the imprinted genes of interest was derived from *Mus musculus castaneus*. Heterozygous and homozygous DMD mutant mice were obtained in the predicted Mendelian ratio and were viable and fertile.

Paternal inheritance of the DMD deletion

To determine the effect of the DMD deletion on the expression of imprinted genes, mice that inherited the mutant allele ($H19^{\Delta DMD}$) from the father were first tested for *H19* expression (Fig. 2a). When the livers from neonatal heterozygous mice were analyzed by RNase protection, the normally silent paternal *H19* allele (Fig. 2a, lanes 8–10) was activated to a level of ~60% of that observed for the maternal wild-type allele, whereas *H19* expression from the maternal allele was unaffected (Fig. 2a, lanes 11–13). The analysis of other tissues showed that the level of activation of the mutant paternal *H19* allele varied according to tissue type, with gut derivatives exhibiting a moderate level of activation, whereas in muscle derivatives activation was nearly equivalent to that for liver (data not shown). These results indicate that deletion of the DMD eliminated sequences that were repressive to *H19* gene expression. The deletion did not, however, completely activate *H19* expression to levels observed for the wild-type maternal allele.

Because transcription of the *Igf2* and *H19* genes is linked (Leighton et al. 1995a,b), the effect of the DMD deletion on *Igf2* expression was examined. Paternal transmission of the mutant $H19^{\Delta DMD}$ allele caused repression of the paternally inherited *Igf2* gene (Fig. 2b, cf. lanes 10–12 and lanes 7–9). When the level of paternal allele expression in the liver of neonatal heterozygous mice was compared to that of wild-type littermates, a

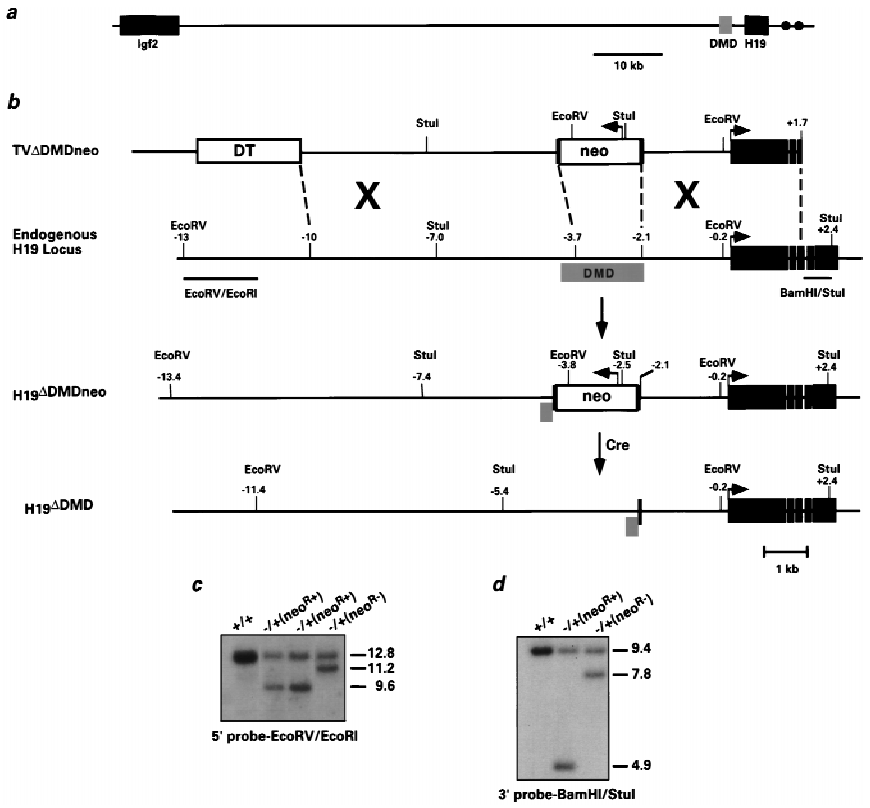

Figure 1. Deletion of the *H19* differentially methylated domain in ES cells. (*a*) The positions of *Igf2* and *H19* relative to the DMD on mouse chromosome 7 are indicated. The gray box corresponds to the 2-kb DMD, which is located −2 to −4 kb relative to the start of *H19* transcription. (●) The endodermal enhancers located at +9 and +11 kb. (*b*) From *top* to *bottom*: the linearized targeting vector, the endogenous *H19* locus, the targeted *H19* locus ($H19^{\Delta DMDneo}$), and the targeted *H19* locus after removal of PGK–*neo* using CRE–*loxP* recombination ($H19^{\Delta DMD}$). The linearized vector includes Bluescript II KS (thick line), the diphtheria toxin A gene (open box, DT), PGK–*neo* (open box, neo) flanked by loxP sites (black vertical bars), 5′ *H19* sequence (thin black line) and *H19* gene sequence extending into the third exon (solid boxes). Arrows indicate direction of transcriptional orientation of PGK–*neo* and *H19*. The positions of the restriction sites and the external probes (*Eco*RV/*Eco*RI and *Bam*HI/*Stu*I) used to analyze the targeted clones are indicated. (*c*,*d*) ES cell clones were screened by Southern blot analysis for the targeting event. Genomic DNA was digested with *Eco*RV and hybridized to the 5′ probe *Eco*RV/*Eco*RI (*c*) or with *Stu*I and hybridized to the 3′ probe *Bam*HI/*Stu*I (*d*). The DNA samples shown include the parental ES cell DNA (+/+), targeted clones with the *neo*^{r} gene (neo^{R+}), and a targeted clone in which the *neo*^{r} gene was excised (neo^{R-}). Molecular sizes (in kb) are indicated to the *right*. Of the 85 G418-resistant clones analyzed, four were correctly targeted to the *H19* locus.

66% reduction in *Igf2* RNA was observed (Fig. 2d). As noted for *H19*, the reduction in *Igf2* expression varied according to tissue (data not shown). Consistent with the decrease in *Igf2* expression, the weights of the heterozygous littermates were on average 93% that of their wild-type littermates. Whereas reduction of *Igf2* expression in liver is concordant with experiments proving that *H19* and *Igf2* share enhancers, it is striking that the level of activation of *H19* from the mutant paternal allele was equivalent roughly to the reduction of *Igf2* expression on the same allele.

Maternal inheritance of the DMD deletion

The effect of maternal transmission of the DMD mutation was also tested for *H19* and *Igf2* expression. Surprisingly, transmission of the mutant $H19^{\Delta DMD}$ allele through the maternal germ line resulted in the reduced expression of the *H19* gene (Fig. 2a, cf. lanes 4–7 with lanes 1–3). When quantified by RNase protection, the expression of *H19* in neonatal livers was approximately half that observed in wild-type littermates (Fig. 2c). To determine if *Igf2* was affected by the maternally derived DMD mutation, allelic *Igf2* expression levels were assayed. The normally silent maternal *Igf2* allele was activated to about one-third the level of the wild-type paternal allele and expression from the wild-type paternal allele was unaffected (Fig. 2b, lanes 2–6). Additionally, when compared to their wild-type littermates, the mice that inherited the mutant allele maternally were on average 17% larger, which is consistent with activation of maternal *Igf2*. Thus, a reduction in the level of *H19* expression on the mutant maternal allele was accompanied by an activation of the maternally derived *Igf2* gene and a slight increase in weight. Because the coordinated expression of *H19* and *Igf2* was also observed upon paternal transmission of the mutation, these results indicate that deletion of the DMD resulted in a true competition for the endodermal enhancers. These results additionally demonstrate that the DMD has a previously unsuspected positive regulatory function for the exclusive expression of the maternal *H19* allele.

Methylation analysis of the targeted H19 *alleles*

We have proposed that the DMD harbors an imprinting mark in the form of paternal-specific methylation (Tremblay et al. 1995, 1997). Because not all of the differentially methylated sequences at the *H19* locus were removed by the DMD deletion, it was of interest to determine the effect of the deletion on the methylation of the remaining CpG dinucleotides. The CpG dinucleotides located in the promoter-proximal region and the 5′ portion of the *H19* structural gene are preferentially

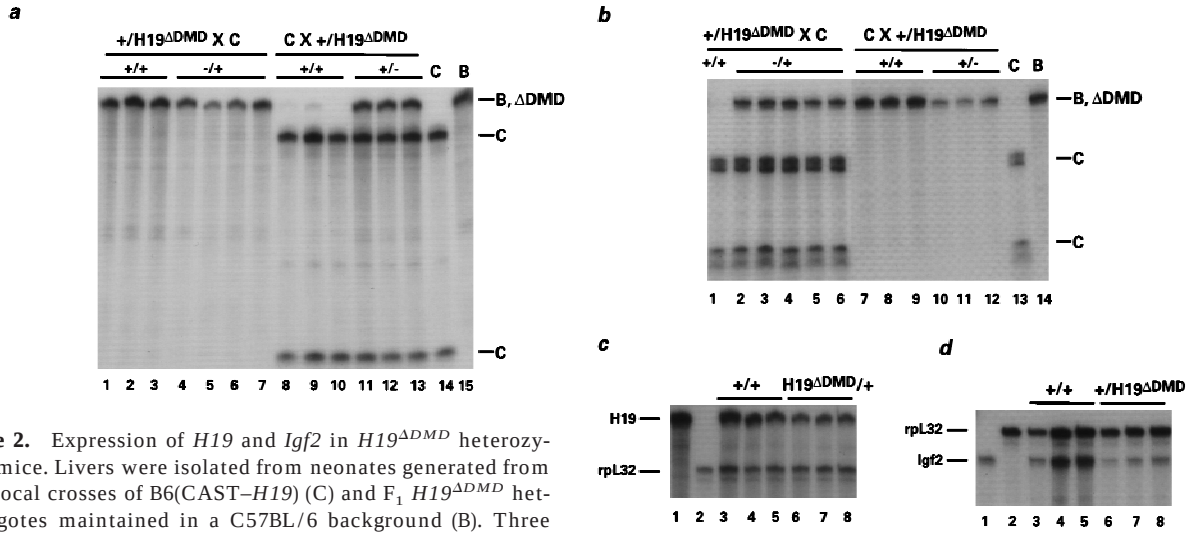

Figure 2. Expression of *H19* and *Igf2* in $H19^{\Delta DMD}$ heterozygous mice. Livers were isolated from neonates generated from reciprocal crosses of B6(CAST–*H19*) (C) and F_1 $H19^{\Delta DMD}$ heterozygotes maintained in a C57BL/6 background (B). Three micrograms of total RNA was analyzed using an allele-specific RNase protection assay. The C-, B-, and ΔDMD-specific protected fragments are designated. (*a*) *H19* expression when $H19^{\Delta DMD}$ was inherited from the mother (lanes *1–7*) or the father (lanes *8–13*). When the mother was heterozygous for the mutation, the maternal allele (B, ΔDMD) was expressed in wild-type newborn mice (+/+, lanes *1–3*) and expressed at a reduced level in mutant (−/+, lanes *4–7*) newborn mice. In 5-day-old littermates generated from paternal heterozygotes, the maternal allele (C) is expressed in wild-type mice (+/+, lanes *8–10*), whereas mutant mice express both alleles (+/−, lanes *11–13*). The relative ratio of paternally to maternally derived *H19* RNA is 0.615, 0.586, and 0.575 (lanes *11–13*, respectively). Note that a low level of expression of the paternal allele (<0.5%) was detected in wild-type mice (lanes *8,9*) as observed previously (Leighton et al. 1995a). Control liver RNA isolated from 4-day-old B6(CAST–*H19*) and 5-day-old C57BL/6 mice was analyzed in lanes *14* and *15*, respectively. (*b*) *Igf2* expression when the $H19^{\Delta DMD}$ allele is maternally (lanes *1–6*) or paternally derived (lanes *7–12*). Three-day-old mice generated from maternal heterozygotes expressed the paternal allele (C) when wild-type for the mutation (+/+, lane *1*) and expressed both alleles when heterozygous for the mutation (−/+, lanes *2–6*). The relative ratio of maternally to paternally derived *Igf2* RNA is 0.373, 0.315, 0.317, 0.338, and 0.370 (lanes *2–6*, respectively). In 5-day-old littermates generated from paternal heterozygotes, the paternal allele is expressed exclusively in wild-type mice (+/+, lanes *7–9*) and expressed at a reduced level in mutant mice (+/−, lanes *10–12*). Control liver RNAs as described in *a* are assayed in lanes *13* and *14*. (*c*) The expression of *H19* is analyzed relative to the expression of *rpL32* when the $H19^{\Delta DMD}$ allele is transmitted by the mother. RNA from wild-type (+/+, lanes *3–5*) and mutant ($H19^{\Delta DMD}$/+, lanes *6–8*) 5-day-old littermates was assayed with *H19* and *rpL32* probes. The ratio of *H19* to *rpL32* RNA is as follows: 2.72, 2.85, 1.60, 1.14, 1.34, and 1.04 (lanes *3–8*, respectively). Neonatal liver RNA is assayed with the *H19* or *rpL32* probes alone in lanes *1* and *2*, respectively. (*d*) The expression of *Igf2* was analyzed relative to *rpL32* when the $H19^{\Delta DMD}$ allele was transmitted by the father. RNA from wild-type (+/+, lanes *3–5*) and mutant (+/$H19^{\Delta DMD}$, lanes *6–8*) newborn littermates is assayed with the *Igf2* and *rpL32* probes. The ratio of *Igf2* to *rpL32* RNA is as follows: 0.465, 0.502, 0.536, 0.150, 0.189, and 0.165 (lanes *3–8*, respectively). Neonatal liver RNA was assayed with the *Igf2* or *rpL32* probes alone in lanes *1* and *2*, respectively. Total RNA levels for the wild-type and heterozygous mutants were confirmed by Northern analysis (data not shown).

methylated on the paternal allele late in gestation [see Fig. 3d, sites between −500 and +501 bp (Bartolomei et al. 1993; Brandeis et al. 1993; Ferguson-Smith et al. 1993; Tremblay et al. 1997)]. In contrast, the 3′ portion of the *H19* structural gene is equally methylated on both alleles [see Fig. 3d, sites downstream of +501 bp (Ferguson-Smith et al. 1993)], as are sites 5′ of the 2-kb DMD [Fig. 3d, upstream of −4000 bp (Tremblay et al. 1997)]. To determine whether the methylation of the *H19* promoter and structural gene was affected by the mutation, neonatal liver DNA from reciprocal heterozygotes was digested with *Pvu*II and *Stu*I and the methylation-sensitive restriction enzyme *Hpa*II and subjected to Southern analysis (Southern 1975). The wild-type *M. castaneus* allele lacks a *Pvu*II site, which enabled the distinction between the mutant C57BL/6 *H19* allele (3.2 kb) and the wild-type *M. castaneus H19* allele (3.4 kb) (Bartolomei et al. 1993). When the mutation was transmitted to the progeny by the mother, the methylation of the *H19* promoter and structural gene appeared unaffected (Fig. 3b, cf. lanes 4 and 6). In contrast, the deletion of the DMD on the paternally inherited allele resulted in the hypomethylation of the *Hpa*II sites in the promoter region (Fig. 3b, *Pvu*II/*Stu*I fragment in lanes 8 and 10). Similarly, a *Hha*I site in the promoter was not methylated on the mutant paternal allele (data not shown). These results were consistent with methylation analysis in homozygous mutant animals in which the promoter was hypomethylated on both alleles (Fig. 3b, lane 13). Thus, deletion of the DMD from the paternal allele was accompanied by a loss of methylation in the sequences surrounding the promoter, causing the mutant paternal allele to resemble the wild-type maternal allele (Fig. 3d).

Next, we examined the methylation status of upstream CpG dinucleotides that remained on the mutant allele (Fig. 3a, sites between −4500 and −500 bp). The *Hha*I site located immediately 5′ to the deletion and the two *Hha*I sites located between the promoter and the

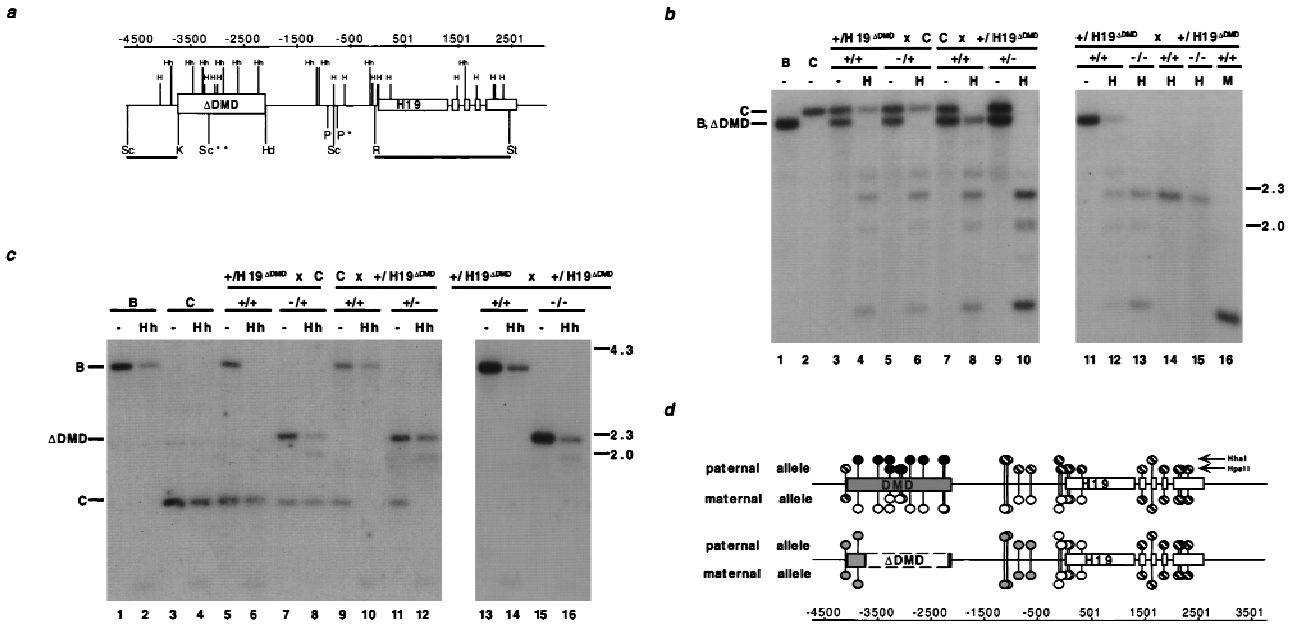

Figure 3. Methylation analysis of *H19* in heterozygous and homozygous DMD mutant mice. (*a*) The location of the *Hpa*II (H) and *Hha*I (Hh) sites with respect to the deleted DMD sequence. The 5′ *H19* DMD sequence, deleted between the *Kpn*I (K) and *Hin*dIII (Hd) sites, and *H19* are represented by boxed regions. (P) *Pvu*II; (R) *Eco*RI; (St) *Stu*I; (Sc) *Sac*I. (*) The polymorphic *Pvu*II site that is found in C57BL/6J and $H19^{\Delta DMD}$; (**) the polymorphic *M. castaneus Sac*I site. The RSt probe used in *b* and the ScK probe used in *c* are indicated *beneath* the line. The position of the sites, relative to the start of transcription, are indicated (in bp) *above* the gene line. (*b*) The methylation status of *Hpa*II sites in the *H19 Pvu*II/*Stu*I fragment is assessed with the RSt probe. DNA from C57BL/6J (B) mice, B6(CAST–*H19*) mice (C), progeny of a $H19^{\Delta DMD}$ heterozygous female mated to a B6(CAST–*H19*) male (lanes *3–6*), progeny from a B6(CAST–*H19*) female mated to a $H19^{\Delta DMD}$ heterozygous male (lanes *7–10*) and progeny of a $H19^{\Delta DMD}$ heterozygous female mated to a $H19^{\Delta DMD}$ heterozygous male (lanes *11–16*) were analyzed. DNA was digested with *Pvu*II and *Stu*I and, in lanes indicated, *Hpa*II (H) or *Msp*I (M). The genotypes of the assayed DNA from the specific mating are indicated above the lanes. DNA from neonatal livers (lanes *1–13,16*) and adult sperm (lanes *14,15*) were assayed. The *M. castaneus*-specific *Pvu*II/*Stu*I fragment (C, 3.4 kb) and the C57BL/6 and $H19^{\Delta DMD}$-specific *Pvu*II/*Stu*I fragment (B, ΔDMD, 3.2 kb) are noted at *left*, with size markers in kb shown at *right*. (*c*) DNA from mice described in *b* was analyzed for *Hha*I methylation in the 5′ *H19 Sac*I fragment using the ScK probe. DNA was digested with *Sac*I and, in lanes indicated, *Hha*I (Hh). The genotypes of the DNA samples are indicated *above* the lanes. The C57BL/6J (3.8 kb), B6(CAST–*H19*) (1.5 kb) and the $H19^{\Delta DMD}$ (2.2 kb)-specific *Sac*I fragments are indicated at *left*. (*d*) Summary of the parental-specific methylation status of *Hpa*II and *Hha*I sites on wild-type (*top* line) vs. $H19^{\Delta DMD}$ (*middle* line) alleles. The taller and shorter lollipops represent the *Hha*I and the *Hpa*II sites, respectively. (Solid circles) Fully methylated sites; (open circles) unmethylated sites; (striped circles) sites that are methylated on a subset of the alleles, as determined from previous studies (bisulfite sequence and Southern analyses) and data presented herewith; (shaded circles) sites that are partially methylated. The paternal-specific methylation status is presented above each allele; the maternal-specific methylation status is presented below each allele.

DMD were analyzed using *Sac*I polymorphic fragments (Fig. 3a). In wild-type animals, the sites were hypermethylated on the paternal allele but hypomethylated on the maternal allele (Fig. 3c, lanes 5,6,9,10). However, the mutant $H19^{\Delta DMD}$ allele was hypermethylated whether it was maternally or paternally transmitted (Fig. 3c, ΔDMD *Sac*I fragment, lanes 7 and 8 and 11 and 12, respectively). This hypermethylation of the mutant allele was also evident in homozygous mutant animals (Fig. 3c, lanes 15,16). The remaining *Hpa*II sites in this upstream region were also hypermethylated on both mutant alleles (data not shown). Thus, whereas the DMD deletion was associated with the hypomethylation of cytosine residues surrounding the promoter, CpG dinucleotides located upstream from the promoter were partially methylated on the mutant alleles (Fig. 3c and data not shown). Taken together, these results indicate that the methylation status of the mutant alleles reflected neither the maternal nor paternal wild-type pattern (Fig. 3d). Rather, the mutant allelic methylation pattern was intermediate between the two wild-type parental alleles and no longer parental-specific.

We also compared the methylation status of sperm DNA isolated from wild-type and homozygous mutant adult males generated from F_1 heterozygous intercrosses. The methylation state of the *H19* promoter, structural gene, and remaining 5′ sequence was unchanged with the removal of the DMD sequence. Specifically, the wild-type and ΔDMD sperm DNA were similarly unmethylated in the *H19* promoter region (Fig. 3b, lanes 14 and 15) and were similarly methylated at *Hha*I sites immediately 5′ and 3′ of the deleted sequence (data not shown). These data indicate that removal of DMD sequence did not perturb the acquisition of the sperm-specific methylation pattern in the remaining *H19* sequence.

Analysis of H19$^{\Delta DMDneo}$ *alleles*

The experiments described above used mice in which the *neo*^{r} gene was excised. To determine if the perturbation of imprinted gene expression was caused solely by the absence of the DMD or if the spacing change imposed by the deletion was responsible for altered gene-expression patterns, mice in which the *neo*^{r} gene remained at the *H19* locus were examined. Because the size of the *neo*^{r} gene was similar to that of the deleted DMD fragment, inclusion of the *neo*^{r} gene preserved spacing of the *H19* upstream elements. As observed for the *H19*$^{\Delta DMD}$ alleles, both the *H19* and *Igf2* genes were expressed on the maternal and paternal *H19*$^{\Delta DMDneo}$ alleles in neonatal liver (Fig. 4). The *neo*^{r} gene did not affect *H19* expression levels on either parental allele (Fig. 4a, data not shown), supporting the proposed role of the DMD as both a positive and negative regulator of *H19* gene expression. However, the presence of the *neo*^{r} gene caused a less dramatic increase in the expression of *Igf2* on the mutant maternal allele (Fig. 4b, lanes 2,3). That is, in the presence of the *neo*^{r} gene, *Igf2* was activated to ~6% that of the wild-type paternal allele, whereas in the absence of the *neo*^{r} gene, *Igf2* expression on the mutant maternal allele increased to an average of one-third the level of the wild-type paternal allele (Fig. 4b, lanes 1–3 and 4–6, respectively). These results suggest that the *neo*^{r} gene interfered with the activation of *Igf2* on the mutant maternal allele and are consistent with studies of regulatory elements at other loci demonstrating that the *neo*^{r} gene regulatory elements affected gene expression (Fiering et al. 1995).

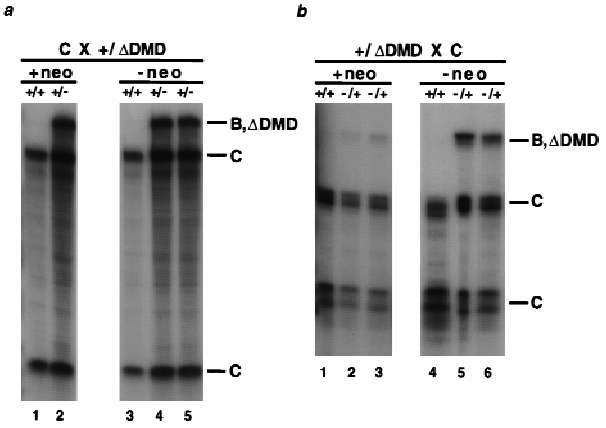

Figure 4. Expression of *H19* and *Igf2* in *H19*$^{\Delta DMD}$ and *H19*$^{\Delta DMDneo}$ mice. The genotypes are noted *above* the lanes and the parental identity of protected fragments are indicated to the right. Neonatal liver RNA (3 µg) is analyzed using allele-specific RNase protection assays. (*a*) *H19* expression in paternal heterozygotes. The RNA isolated from a wild-type and a mutant littermate, generated from mating a B6(CAST–*H19*) female with a heterozygous *H19*$^{\Delta DMDneo}$ male, is assayed in lanes *1* and *2*, respectively. The RNA isolated from the progeny of a mating between a B6(CAST–*H19*) female and a heterozygous *H19*$^{\Delta DMD}$ male is assayed in lanes *3–5*. (*b*) *Igf2* expression in maternal heterozygotes. RNA from wild-type and mutant +neo littermates (lanes *1* and *2* and *3*, respectively) and wild-type and mutant −neo littermates (lanes *4* and *5* and *6*, respectively) produced from the reciprocal mating performed in *a* is assayed.

The imprinting of the *neo*^{r} gene was also assessed in RNA isolated from livers of heterozygous and homozygous *H19*$^{\Delta DMDneo}$ neonatal mice. Northern blot analysis showed that the *neo*^{r} expression levels were similar in the maternal and paternal *H19*$^{\Delta DMDneo}$ heterozygous mutants and twofold higher in the homozygous mutants (data not shown), demonstrating *neo*^{r} expression was not imprinted. Thus, in contrast to previous experiments in which the *neo*^{r} gene was used to replace the *H19* transcription unit and was imprinted (Ripoche et al. 1997), the sequences remaining at the *H19*$^{\Delta DMD}$ locus were not sufficient to imprint the *neo*^{r} gene.

Discussion

We proposed previously that paternal-specific DNA methylation in the region located from −2 to −4 kb relative to the start of *H19* transcription is involved in the imprinting of the mouse *H19* gene (Tremblay et al. 1997). Absence of this region in a normally imprinted mouse transgene results in parental-independent expression and hypomethylation of the derivative transgene (Elson and Bartolomei 1997), indicating that the DMD is crucial for suppression of a paternally transmitted transgene. This element also has unique properties in *Drosophila* where it acts as a silencer, despite the absence of DNA methylation in the *Drosophila* genome (Lyko et al. 1997).

To test the role of the DMD at the endogenous *H19* gene locus, we have deleted most of this region using gene-targeting technology. Paternal transmission of the mutant allele resulted in activation of *H19* expression, a concomitant reduction in *Igf2* expression, and a reduction in methylation of the remaining CpG dinucleotides at the *H19* locus (Fig. 5). These results are consistent with the transgenic experiments and support the hypothesis that the DMD represses transcription of the paternally derived *H19* allele. The negative regulatory role of the paternally derived DMD is likely caused by its hypermethylation that could either act directly by preventing the binding of factors that establish a transcriptionally competent state or could act indirectly through the methyl-CpG-binding protein MeCP2, or other unknown proteins with analogous activities, which subsequently recruits histone deacetylases and represses transcription (Jones et al. 1998b; Nan et al. 1998).

A new finding of this study was the observed decrease in *H19* expression together with the concomitant activation of *Igf2* upon maternal transmission of the mutant allele, suggesting that the DMD also influences transcription of *H19* on the maternal allele positively (Fig. 5). Indeed, chromatin studies of the *H19* locus have shown that the DMD is hypersensitive to nucleases exclusively on the maternal chromosome, supporting the concept of a novel maternally derived positive role for this element (Hark and Tilghman 1998). A number of mechanisms could lead to this positive regulatory function. First, the unmethylated DMD might bind transcription factors

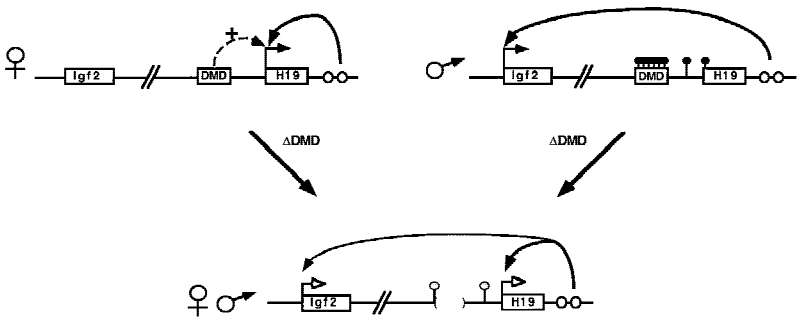

Figure 5. A model for DMD-regulated *H19* and *Igf2* imprinting based on the analysis of neonatal liver. The maternal and paternal wild-type alleles are represented with parental-specific gene expression (horizontal arrows) and *H19* paternal-specific methylation (filled-in circles above the locus). The *H19* and *Igf2* genes and the DMD are depicted as boxes and endodermal enhancers as open circles. The deletion of the DMD (bordered by parentheses) on the maternal or the paternal allele results in expression of both genes as depicted at *bottom*. In addition, 5′ *H19* sequence is similarly methylated on both alleles (shaded circles above 5′ *H19* sequence). The model illustrates the following properties of the DMD. (1) The DMD positively affects maternal *H19* expression (broken arrow); when it is deleted, maternal *H19* expression is reduced (open arrowheads). (2) The DMD contributes to silencing of the paternal *H19* allele. (3) Presence of the DMD is required for reciprocal imprinting of *Igf2*. In ΔDMD mice, reduced *H19* expression on the maternal allele is accompanied by activated *Igf2* expression, and activated *H19* expression from the paternal allele is accompanied by reduced *Igf2* expression, consistent with previous proposals that the endodermal enhancers are shared. (4) Paternal-specific methylation is maintained in the presence of DMD. (5) The DMD serves as the mark that distinguishes the parental alleles of *H19*.

that promote the expression of *H19*. In the case of the mutant maternal allele, the decreased expression of *H19* may be caused by the loss of positive transcriptional elements rendering *H19* less effective in utilizing the endoderm-specific enhancers. These enhancers are then free to drive the expression of *Igf2*. Thus, although the DMD is not required for transgenic *H19* expression (Pfeifer et al. 1996; Elson and Bartolomei 1997), possibly because of the absence of the competing *Igf2* gene, it appears to be essential for the optimal and exclusive expression of *H19* at the endogenous locus. Second, the maternally derived DMD may form a unique chromatin configuration that promotes transcriptional activity. Third, the DMD could act as a selector that directs transcription either toward *H19* or *Igf2*. Fourth, the DMD may function to repress *Igf2* transcription on the maternal allele, thereby indirectly affecting *H19* expression. Thus, in the absence of the DMD on the maternal allele, *Igf2* expression is derepressed, which reduces access of the enhancers to *H19*. Finally, Tilghman and colleagues have suggested that the DMD acts as a domain boundary or a chromatin insulator which isolates the *H19* promoter and endodermal enhancers and blocks the *Igf2* gene from accessing these enhancers on the maternal chromosome (Webber et al. 1998). Originally identified in *Drosophila*, boundary elements insulate a gene and its regulatory elements from position effect variegation and can block gene expression when placed between a gene and its enhancers (Kellum and Schedl 1991, 1992). The proposal that the DMD functions as a domain boundary in mouse is supported by experiments in which *Igf2* is preferentially expressed on maternally derived chromosomes in which the *H19* endoderm enhancers were removed from their normal location and placed between the *H19* and *Igf2* genes and upstream of the DMD (Webber et al. 1998). Although these latter experiments could be explained by distance effects or the placement of the enhancers in a new chromatin environment, taken together, the gene-targeting experiments would argue in favor of the DMD acting as a domain boundary. Formal proof of this model will require the demonstration that the DMD insulates gene expression at a heterologous locus.

The experiments described in this report support the original model proposing that the reciprocal imprinting of the *H19* and *Igf2* genes is mediated by a competition for the shared set of endoderm enhancers [Fig. 5 (Bartolomei and Tilghman 1992)]. Mice harboring the DMD deletion express *H19* and *Igf2* from the mutant chromosome, with enhanced expression of one gene accompanied by a coordinate decrease in the expression of the other gene. The canonical example for this type of regulation is the promoter competition in the chicken β-globin gene complex, where the switch from the embryonic ϵ-globin to the adult β-globin is achieved through a competition for the β-globin enhancer (Choi and Engel 1988; Foley and Engel 1992). Similar to the compensatory expression changes observed in our mutant mice, mutations that attenuated adult β-globin expression were accompanied by an increase in the expression of ϵ-globin (Foley and Engel 1992). Recent experiments by Jones and colleagues indicate that the competition by *H19* and *Igf2* promoters for the endoderm enhancers may not be mediated strictly by the promoters and DMD alone (Jones et al. 1998a). In experiments in which the *H19* transcriptional unit was replaced with the *luciferase* gene, *luciferase* was expressed at variable levels on the paternal allele, whereas the expression and imprinting of *Igf2* was maintained at wild-type levels. One interpretation of these experiments is that the RNA-coding portion of the *H19* gene is also required for linked competition of these genes.

Our study does not address the mechanism by which *H19* and *Igf2* share enhancer elements at the cellular level. For example, in the paternal mutant heterozygote, *H19* and *Igf2* may be expressed simultaneously from the mutant allele. Alternatively, each cell makes a choice: some cells may exclusively express *Igf2* from the mutant paternal allele and other cells may exclusively express *H19*. It is also possible that each cell expresses both

genes from the mutant paternal allele but only one gene is expressed at a given time. The latter is analogous to the flip-flop model of gene regulation that has been proposed to explain how distal control elements allow the simultaneous expression of γ- and β-globin in early development (Wijgerde et al. 1995). Future studies of our mutants at the cellular level will discriminate between these possibilities.

Finally, we have determined that deletion of the DMD on one chromosome does not appear to affect the expression or methylation of the genes on the wild-type chromosome. Unlike experiments showing that *Igf2* transgenes can transactivate the endogenous *Igf2* gene and lead to Beckwith-Wiedemann-related symptoms (Sun et al. 1997), the activation of either *H19* or *Igf2* on the mutant chromosome does not affect the expression of their counterparts on the wild-type chromosome. Furthermore, after three generations of breeding the mutant mice, the only observed phenotypes in animals with alterations in *H19* and *Igf2* expression are subtle size effects that are consistent with the changes in *Igf2* expression. No phenotypic consequences reminiscent of Beckwith-Wiedemann have been noted. Additionally, homozygous mutant animals have no apparent phenotype, possibly because the total expression of *H19* and *Igf2* in the neonatal livers of homozygous animals is similar to that of wild-type animals (data not shown).

In conclusion, we have demonstrated that the DMD has multiple roles in regulating the imprinting of the *H19* gene. Our hypothesis that the differential methylation serves as the allelic mark is strengthened by the observation that deletion of the DMD on both chromosomes renders them indistinguishable by the criteria employed in these studies. As expected, the DMD mediates a repressive effect on the transcription of the paternally derived chromosome, presumably through its hypermethylation. Additionally, we have shown that the DMD permits the exclusive expression of *H19* on the maternal chromosome, possibly through the binding of positive regulatory factors, a unique chromatin configuration, inhibition of *Igf2*, or through the assembly of a domain boundary which prevents access of *Igf2* to the enhancers. Future studies will elucidate the factors responsible for the multiple roles of this complex element.

Materials and methods

Preparation of the targeting vector

A phage clone containing 13.5 kb of 5′ flanking and 1.8 kb of *H19* gene sequence was isolated from a 129Sv/J mouse genomic library in the Lambda FIX II vector (Stratagene). The phage insert was subcloned as two fragments into Bluescript II KS (Stratagene); a *Not*I/*Kpn*I fragment corresponding to 9.8 kb of 5′ flanking *H19* sequence (p9.8N/K) and a *Kpn*I/*Not*I fragment containing the remaining 5′ flanking and *H19* gene sequence (p5.5K/N). The *Kpn*I site is −3.7 kb relative to the start of *H19* transcription and is the 5′ boundary of the DMD-targeting event. To initiate construction of the targeting vector, an *Eco*RI/*Xho*I fragment containing a 2-kb PGK–*neo* loxP flanked cassette was subcloned into Bluescript II KS and the *Xho*I site was eliminated subsequently (ploxPneo–BS). p5.5K/N was then digested with *Hin*dIII, blunted with Klenow, and digested with *Not*I to generate the 3.9-kb *Hin*dIII/*Not*I *H19* fragment that serves as the 3′ arm of the targeting vector. This fragment was subcloned into *Not*I/*Sma*I-digested ploxPneo–BS to generate pneo3′H19. To assemble the target vector the following were simultaneously ligated: a 6.6-kb *Bam*HI/*Kpn*I 5′ *H19* fragment (from p9.8N/K), a 5.9-kb *Kpn*I/*Not*I fragment including loxP–*neo* cassette and 3.9-kb *H19* sequence (from pneo3′H19), and *Not*I/*Bam*HI digested Bluescript II KS. Finally, a 2.3-kb *Sal*I fragment containing a diphtheria toxin A cassette (McCarrick et al. 1993) was ligated to the *Xho*I linearized target vector. The final targeting vector contains a total of 10.1 kb of homology to the *H19* locus (Fig. 1b).

Targeted disruption of the DMD region in ES cells

The vector was linearized at a unique *Not*I site prior to electroporation into ES cells. E14.1 ES cells (Kuhn et al. 1991) were grown on neomycin-resistant mouse embryonic fibroblasts. ES cells (1.5×10^7/ml) were collected in 0.8 ml of phosphate-buffered saline and electroporated with a pulse of 250 V/500 mF (Gene Pulser, Bio-Rad) with 25 μg of linearized targeting vector. Following a 24-hr recovery, the medium was adjusted to 200 μg/ml G418. After 8–10 days growth, G418-resistant colonies were isolated and expanded, and DNA was prepared. The DNA was digested with *Eco*RV (5′-end confirmation) or *Stu*I (3′-end confirmation) and size fractionated on 0.75% and 1.0% agarose gels, respectively. DNA was transferred to nitrocellulose (Southern 1975) and hybridized to nick-translated external probes (Rigby et al. 1977). The *Eco*RV/*Eco*RI probe was used for 5′-end confirmation and the *Bam*HI/*Stu*I probe was used for 3′-end confirmation (Fig. 1b).

The *neo*^{r} cassette was removed by transiently transfecting two independent ΔDMD^{neo} ES cell lines with 25 μg of a plasmid encoding the Cre recombinase (Sauer and Henderson 1990). Correctly excised clones were verified by digestion with *Stu*I or *Eco*RV, as described above, and by a 350-bp PCR product that was amplified using primers that flank the ΔDMD mutation. The forward primer was 5′-ATCCAGGAGGCATCCGAATT-3′ and the reverse primer was 5′-GTGTCACAAATGCCTGATCC-3′.

Cells from targeted ES cell clones (with and without the *neo*^{r} gene) were injected into C57BL/6J blastocysts, and the blastocysts were transferred to pseudopregnant female mice. To determine if germ-line transmission of the mutant allele had occurred, chimeras were bred with C57BL/6J mice, and DNA was isolated from tail biopsies of progeny. The Southern blot and PCR analyses described above were used to genotype the mice. To analyze allelic expression and methylation patterns, the heterozygous mutant mice were bred to the B6(CAST–*H19*) strain of mice (Tremblay et al. 1995). These mice have *M. castaneus H19* and *Igf2* alleles on a C57BL/6 background. For F_1 hybrid mice, the maternal parent is designated first.

RNA isolation and analysis

Total RNA was prepared from various staged mouse tissues by the lithium chloride method (Auffray and Rougeon 1980). The RNase protection assays that were used to detect *H19* (Bartolomei et al. 1991; Brunkow and Tilghman 1991), *Igf2* (Leighton et al. 1995a), and *rpL32* (Dudov and Perry 1984) gene expression were performed as described previously. Products were resolved on a 7.0% acrylamide/7 M urea gel.

For quantitation, RNase protection gels were exposed to storage phosphor screens that were scanned on a Storm 840 PhosphorImager (Molecular Dynamics). Band intensities were calculated using ImageQuant Version 1.0 (Molecular Dynamics). After pseudocolor enhancement of the image, bands of interest were traced using the freehand drawing tool. The median pixel values of individual segment boundaries were used as the background values. In all cases, RNase protection assays of the deletion allele produce one protected fragment, whereas assays of the wild-type *M. castaneus* allele produce two protected fragments. In samples in which biallelic expression was observed, the value of the mutant protected fragment was quantified relative to the two fragments corresponding to the wild-type B6(CAST–*H19*) allele. The levels of *H19* RNA in ΔDMD maternal heterozygotes and *Igf2* RNA in ΔDMD paternal heterozygotes were quantified relative to wild-type levels using rpL32 as an internal control.

DNA isolation and methylation analysis

DNA was isolated from tissues and sperm as described previously (Bartolomei et al. 1993). Genomic DNA (10 µg) was digested with *Pvu*II and *Stu*I in combination with *Hpa*II or *Msp*I to analyze the methylation of the *H19* structural gene or with *Sac*I and *Hha*I to analyze the methylation of upstream sequences. The probes used for the respective analyses were the 2.5-kb *Eco*RI–*Stu*I (RSt) fragment and the 0.9-kb *Sac*I–*Kpn*I (ScK) 5′ fragment (Fig. 3a).

Acknowledgments

We thank J. Richa and the University of Pennsylvania Transgenic Core Facility for the production of chimeric mice. We thank M. Malim, S. Liebhaber, A. Webber, K. Tremblay, and members of the lab for critical reviews of the manuscript. We are grateful to A. Hark and S.M. Tilghman for communication of results prior to publication. This work was supported by U.S. Public Service grant GM51279 and the Howard Hughes Medical Institute. J.L.T. was supported by National Research Service Award postdoctoral fellowship GM18458.

The publication costs of this article were defrayed in part by payment of page charges. This article must therefore be hereby marked 'advertisement' in accordance with 18 USC section 1734 solely to indicate this fact.

References

Auffray, C. and F. Rougeon. 1980. Purification of mouse immunoglobulin heavy-chain messenger RNAs from total myeloma tumor RNA. *Eur. J. Biochem.* **107:** 303–314.

Barlow, D.P. 1997. Competition—a common motif for the imprinting mechanism. *EMBO J.* **16:** 6899–6905.

Bartolomei, M.S. and S.M. Tilghman. 1992. Parental imprinting of mouse chromosome 7. *Semin. Dev. Biol.* **3:** 107–117.

———. 1997. Genomic imprinting in mammals. *Annu. Rev. Genet.* **31:** 493–525.

Bartolomei, M.S., S. Zemel, and S.M. Tilghman. 1991. Parental imprinting of the mouse H19 gene. *Nature* **351:** 153–155.

Bartolomei, M.S., A.L. Webber, M.E. Brunkow, and S.M. Tilghman. 1993. Epigenetic mechanisms underlying the imprinting of the mouse *H19* gene. *Genes* & *Dev.* **7:** 1663–1673.

Brandeis, M., T. Kafri, M. Ariel, J.R. Chaillet, J. McCarrey, A. Razin, and H. Cedar. 1993. The ontogeny of allele-specific methylation associated with imprinted genes in the mouse. *EMBO J.* **12:** 3669–3677.

Brunkow, M.E. and S.M. Tilghman. 1991. Ectopic expression of the *H19* gene in mice causes prenatal lethality. *Genes* & *Dev.* **5:** 1092–1101.

Caspary, T., M.A. Cleary, C.C. Baker, X.-J. Guan, and S.M. Tilghman. 1998. Multiple mechanisms regulate imprinting of the mouse distal chromosome 7 gene cluster. *Mol. Cell. Biol.* **18:** 3466–3474.

Choi, O.-R.B. and J.D. Engel. 1988. Developmental regulation of β-globin switching. *Cell* **55:** 17–26.

DeChiara, T.M., E.J. Robertson, and A. Efstratiadis. 1991. Parental imprinting of the mouse insulin-like growth factor II gene. *Cell* **64:** 849–859.

Dudov, K.P. and R.P. Perry. 1984. The gene encoding the mouse ribosomal protein L32 contains a uniquely expressed intron containing gene and an unmutated processed gene. *Cell* **37:** 457–468.

Elson, D.A. and M.S. Bartolomei. 1997. A 5′ differentially methylated sequence and the 3′ flanking region are necessary for *H19* transgene imprinting. *Mol. Cell. Biol.* **17:** 309–317.

Ferguson-Smith, A.S., H. Sasaki, B.M. Cattanach, and M.A. Surani. 1993. Parental-origin-specific epigenetic modification of the mouse *H19* gene. *Nature* **362:** 751–754.

Fiering, S., S. Epner, K. Robinson, Y. Zhuang, A. Telling, M. Hu, D.I. Martin, T. Enver, T.J. Ley, and M. Groudine. 1995. Targeted deletion of 5′HS2 of the murine β-globin LCR reveals that it is not essential for the proper regulation of the beta-globin locus. *Genes* & *Dev.* **15:** 2203–2213.

Foley, K.P. and J.D. Engel. 1992. Individual stage selector element mutations lead to reciprocal changes in β- vs. ϵ-globin gene transcription: Genetic confirmation of promoter competition during globin gene switching. *Genes* & *Dev.* **6:** 730–744.

Giddings, S.J., C.D. King, K.W. Harman, J.F. Flood, and L.R. Carnaghi. 1994. Allele specific inactivation of insulin 1 and 2 in the mouse yolk sac indicates imprinting. *Nat. Genet.* **6:** 310–313.

Gould, T.D. and K. Pfeifer. 1998. Imprinting of mouse *Kvlqt1* is developmentally regulated. *Hum. Mol. Genet.* **7:** 483–487.

Guillemot, F., T. Caspary, S.M. Tilghman, N.G. Copeland, D. J. Gilbery, N. A. Jenkins, D.J. Anderson, A.L. Joyner, J. Rossant, and A. Nagy. 1995. Genomic imprinting of Mash-2, a mouse gene required for trophoblast development. *Nat. Genet.* **9:** 235–241.

Hark, A.T. and S.M. Tilghman. 1998. Chromatin conformation of the *H19* epigenetic mark. *Hum. Mol. Genet.* (in press).

Hatada, I. and T. Mukai. 1995. Genomic imprinting of p57/KIP2, a cyclin-dependent kinase inhibitor, in mouse. *Nat. Genet.* **11:** 204–206.

Jones, B.K., J.M. Levorse, and S.M. Tilghman. 1998a. *Igf2* imprinting does not require its own DNA methylation or *H19* RNA. *Genes* & *Dev.* **12:** 2200–2207.

Jones, P.L., G.J.C. Veenstra, P.A. Wade, D. Vermaak, S.U. Kass, N. Landsberger, J. Strouboulis, and A.P. Wolffe. 1998b. Methylated DNA and MeCP2 recruit histone deacetylase to repress transcription. *Nat. Genet.* **19:** 187–191.

Kellum, R. and P. Schedl. 1991. A position-effect assay for boundaries of higher order chromatin domains. *Cell* **64:** 941–950.

———. 1992. A group of scs elements function as domain boundaries in an enhancer-blocking assay. *Mol. Cell. Biol.* **12:** 2424–2431.

Kuhn, R., K. Rajewsky, and W. Muller. 1991. Generation and analysis of interleukin-4 deficient mice. *Science* **254:** 707–710.

Leighton, P.A., R.S. Ingram, J. Eggenschwiler, A. Efstratiadis, and S.M. Tilghman. 1995a. Disruption of imprinting caused

by deletion of the *H19* gene region in mice. *Nature* **375:** 34–39.

Leighton, P.A., J.R. Saam, R.S. Ingram, C.L. Stewart, and S.M. Tilghman. 1995b. An enhancer deletion affects both *H19* and *Igf2* expression. *Genes* & *Dev.* **9:** 2079–2089.

Li, E., C. Beard, and R. Jaenisch. 1993. Role for DNA methylation in genomic imprinting. *Nature* **366:** 362–365.

Lyko, F., J.D. Brenton, M.A. Surani, and R. Paro. 1997. An imprinting element from the mouse *H19* locus functions as a silencer in *Drosophila*. *Nat. Genet.* **16:** 171–173.

McCarrick, J.W.I., J.R. Parnes, R.H. Seong, D. Solter, and B.B. Knowles. 1993. Positive-negative selection gene targeting with the diphtheria toxin A-chain gene in mouse embryonic stem cells. *Transgen. Res.* **2:** 183–190.

Monk, M., M. Boubelik, and S. Lehnert. 1987. Temporal and regional changes in DNA methylation in the embryonic, extraembryonic and germ cell lineages during mouse embryo development. *Development* **99:** 371–382.

Nan, X., H.-H. Ng, C.A. Johnson, C.D. Laherty, B.M. Turner, R.N. Eisenman, and A. Bird. 1998. Transcriptional repression by the methyl-CpG-binding protein MeCP2 involves a histone deacetylase complex. *Nature* **393:** 386–389.

Nicholls, R.D., S. Saitoh, and B. Horsthemke. 1998. Imprinting in Prader-Willi and Angelman Syndromes. *Trends Genet.* **14:** 194–200.

Olek, A. and J. Walter. 1997. The pre-implantation ontogeny of the *H19* methylation imprint. *Nat. Genet.* **17:** 275–276.

Pfeifer, K., P. Leighton, and S.M. Tilghman. 1996. The structural gene of *H19* is required for transgene imprinting. *Proc. Natl. Acad. Sci.* **93:** 13876–13883.

Reid, L.H., C. Davies, P.R. Cooper, S.J. Crider-Miller, S.N. J. Sait, N.J. Nowak, F. Evans, E.J. Stanbridge, P. deJong, T.B. Shows, B.E. Weissman, and M.J. Higgins. 1997. A 1-mb physical map and PAC contig of the imprinted domain in 11p15.5 that contains TAPA1 and the BWSCR1/WT2 region. *Genomics* **43:** 366–375.

Rigby, P.W.J., M. Dieckmann, D. Rhodes, and P. Berg. 1977. Labeling deoxyribonucleic acid to high specific activity *in vitro* by nick translation with DNA polymerase I. *J. Mol. Biol.* **113:** 237–251.

Ripoche, M.-A., K. Chantal, F. Poirier, and L. Dandolo. 1997. Deletion of the H19 transcription unit reveals the existence of a putative imprinting control element. *Genes* & *Dev.* **11:** 1596–1604.

Sanford, J.P., H.J. Clark, V.M. Chapman, and J. Rossant. 1987. Differences in DNA methylation during oogenesis and spermatogenesis and their persistance during early embryogenesis in the mouse. *Genes* & *Dev.* **1:** 1039–1046.

Sauer, B. and N. Henderson. 1990. Targeted insertion of exogenous DNA into the eukaryotic genome by the cre recombinase. *New Biol.* **2:** 441–449.

Southern, E.M. 1975. Detection of specific sequences among DNA fragments separated by gel electrophoresis. *J. Mol. Biol.* **98:** 503–5l7.

Sun, F.-L., W.L. Dean, G. Kelsey, N.D. Allen, and W. Reik. 1997. Transactivation of *Igf2* in a mouse model of Beckwith-Wiedemann syndrome. *Nature* **389:** 809–815.

Tremblay, K.D., K.L. Duran, and M.S. Bartolomei. 1997. A 5′ 2-kilobase-pair region of the imprinted mouse *H19* gene exhibits exclusive paternal methylation throughout development. *Mol. Cell. Biol.* **17:** 4322–4329.

Tremblay, K.D., J.R. Saam, R.S. Ingram, S.M. Tilghman, and M.S. Bartolomei. 1995. A paternal-specific methylation imprint marks the alleles of the mouse *H19* gene. *Nat. Genet.* **9:** 407–413.

Webber, A.L., R.S. Ingram, J.M. Levorse, and S.M. Tilghman. 1998. Location of enhancers is essential for the imprinting of *H19* and *Igf2* genes. *Nature* **391:** 711–715.

Wijgerde, M., F. Grosveld, and P. Fraser. 1995. Transcription complex stability and chromatin dynamics *in vivo*. *Nature* **377:** 209–213.

Yoo-Warren, H., V. Pachnis, R.S. Ingram, and S.M. Tilghman. 1988. Two regulatory domains flank the mouse H19 gene. *Mol. Cell. Biol.* **8:** 4707–4715.

Zemel, S., M.S. Bartolomei, and S.M. Tilghman. 1992. Physical linkage of two mammalian imprinted genes. *Nat. Genet.* **2:** 61–65.